A Spectrum-Aware Clustering for Efficient Multimedia Routing in Cognitive Radio Sensor Networks

Ghalib A. Shah, *Member, IEEE*, Fatih Alagoz, *Member, IEEE*, Etimad A. Fadel, and Ozgur B. Akan, *Senior Member, IEEE*

***Abstract*—Multimedia applications are characterized as delay-sensitive and high-bandwidth stipulating traffic sources. Supporting such demanding applications on cognitive radio sensor networks (CRSNs) with energy and spectrum constraints is a highly daunting task. In this paper, we propose a spectrum-aware cluster-based energy-efficient multimedia (SCEEM) routing protocol for CRSNs that jointly overcomes the formidable limitations of energy and spectrum. Clustering is exploited to support the quality of service (QoS) and energy-efficient routing by limiting the participating nodes in route establishment. In SCEEM routing, the number of clusters is optimally determined to minimize the distortion in multimedia quality that occurs due to packet losses and latency. Moreover, the cluster-head selection is based on the energy and relative spectrum awareness such that non-contiguous available spectrum bands are clustered and scheduled to provide continuous transmission opportunity. Routing employs clustering with hybrid medium access by combining carrier-sense multiple access (CSMA) and time-division multiple access (TDMA). TDMA operates for intracluster transmission, whereas CSMA is used for intercluster routing. Thus, a cross-layer design of routing, i.e., of medium access control (MAC) and physical layers, provides efficient multimedia routing in CRSNs, which is revealed through simulation experiments.**

***Index Terms*—Clustering, cognitive radio sensor networks (CRSN), cross-layer routing, multimedia.**

Manuscript received April 1, 2013; revised August 15, 2013 and November 17, 2013; accepted December 13, 2013. Date of publication January 14, 2014; date of current version September 11, 2014. This work was supported in part by the Turkish Scientific and Technical Research Council under Grant 110E249 and in part by the Turkish National Academy of Sciences through the Distinguished Young Scientist Award Program (TUBA-GEBIP). The review of this paper was coordinated by Prof. J.-Y. Chouinard.

G. A. Shah is with the Al-Khwarizmi Institute of Computer Science, University of Engineering and Technology, Lahore 54890, Pakistan (e-mail: ghalib@kics.edu.pk).

F. Alagoz is with the Department of Computer Engineering, Boğaziçi University, Istanbul 34470, Turkey (e-mail: alagoz@boun.edu.tr).

E. A. Fadel is with the Faculty of Computing and Information Technology, King Abdulaziz University, Jeddah 22254, Saudi Arabia (e-mail: eafadel@kau.edu.sa).

O. B. Akan is with the Next-Generation and Wireless Communication Laboratory, Department of Electrical and Electronics Engineering, Koç University, Istanbul 34450, Turkey and also with Faculty of Computing and Information Technology, King Abdulaziz University, Jeddah 22254, Saudi Arabia (e-mail: akan@ku.edu.tr).

Color versions of one or more of the figures in this paper are available online at http://ieeexplore.ieee.org.

Digital Object Identifier 10.1109/TVT.2014.2300141

I. Introduction

A cognitive radio network (CRN) is formed by advanced radio devices, which observe the radio environment for a suitable band, employ an intelligent agent for decision-making and a frequency-agile radio that can be tuned to a wide range of frequency bands and, eventually, operate on an intelligently selected band. Motivated by the spectrum utilization and regulation issue for exclusive use by the licensed or primary users (PUs), it brings a revolutionary change in this new paradigm by introducing a new class of unlicensed or secondary users (SUs) who can share the spectrum opportunistically without interfering with the primary users. This new paradigm has also been investigated for wireless sensor networks (WSNs) [1] to enjoy the potential benefits of CRs, thus forming CR sensor networks (CRSNs). CRSNs can be utilized in many different application scenarios, for instance, intelligent transportation systems [2], smart grids [4], industrial monitoring [5], surveillance [6], etc. Dynamic spectrum access plays a key role in mitigating the noisy spectrum bands and eases the reconfiguration of spectrum usage. Wireless multimedia sensors have been realized for monitoring and for intelligent transportation in public transport vehicles, such as trains [7]. However, the spectrum utilization issues for multimedia delivery in vehicular networks have not been addressed adequately.

The lack of established infrastructure, network dynamics, and constrained spectrum access privileges, along with the unpredictable band opportunity and the nature of the wireless medium, offer an unprecedented set of challenges in supporting demanding applications over CRSNs. Thus, supporting multimedia applications of traditional wireless multimedia sensor networks (WMSNs) over CRSNs presents many key issues, which are not dealt with in its counterpart WMSN. The multimedia routing protocol for CRSNs should exhibit the following properties.

- *Rate adaptation with opportunistic bandwidth.* The modern variable-rate encoder [25] demands high and variable bandwidth in conjunction with strict delay constraints. This feature of multimedia streams should be best exploited in CRSNs by adapting source rate according to the time-varying available capacity of CRs.
- *Delay and jitter control.* The varying capacity of wireless links in CRSNs deteriorates the performance of a routing protocol in achieving end-to-end delay bound. The strict delay constraint is usually compensated for by setting a

suitable playout deadline to take into account the underlying network bottlenecks [8]. Thus, by setting appropriate deadlines in conjunction with playout time, the multimedia routing protocol should address the significant variation in delay and jitter to ensure the persistent QoS for multimedia applications.

- *Resource constraint.* CRSNs face the challenges of resource limitations inherited from the traditional WSNs, which include mainly power, processing, and memory in addition to the unpredictable time-varying capacity of channels and complexity of CR itself. Therefore, the potential routing protocol should support the efficient resource utilization of sensor nodes.

The mainstream CR research has focused on developing effective spectrum sensing and access techniques for transmission of the unconstrained type of data on infrastructure-based CRNs and, to some extent, for multihop CR ad hoc networks [19]–[22]. Very little effort is made in the literature to support multimedia over multihop CRNs [12], [14], [15]. Generally, centralized approaches [9], [11] are analyzed to provide optimal performance for CR communications. However, recent developments in this field has motivated the investigation of distributed algorithms to provide near optimal efficiency for infrastructureless wireless networks, particularly resource-constrained WSNs. To this end, distributed clustering can efficiently deal with the resource limitations and scalability for densely deployed sensor networks [28].

In this paper, we exploit the clustering algorithm to manage dynamic spectrum access and QoS routing for multimedia CRSNs. A spectrum-aware clustering protocol for energy-efficient multimedia routing (SCEEM) is proposed in which channels are clustered using the spectrum sensing results obtained from each node and the past usage experience. This is based on the phenomenon of scheduling available spectrum over Q slots in a clustering round. Similarly, routing is based on node clustering, in which a cluster head is elected that has higher residual energy and spectrum rank relative to its neighbors. Moreover, routing is integrated with a hybrid time-division multiple-access (TDMA) and carrier-sense multiple-access (CSMA) medium access protocol to relay intracluster and intercluster packets, respectively. In particular, the contributions of SCEEM are threefold. First, it isolates the time and frequency variability of the spectrum for smooth operations of multimedia delivery. Second, it preserves the QoS of each source with graceful degradation. Third, it achieves energy efficiency without compromising the multimedia quality.

An earlier version of this paper appeared in [3]. The remainder of this paper is organized as follows. In Section II, the existing work is investigated for multimedia. The system model is presented in Section III, and the approach is described in Section IV. Performance evaluation is discussed in Section V, and finally, this paper is concluded in Section VI.

II. Related Work

Dynamic spectrum-access protocols for CR ad hoc networks have been explored to some extent, although they cannot be realized for CRSNs since they do not address resource constraints of sensor nodes. Nevertheless, multimedia support in CR ad hoc networks or CRSNs is unexplored. In [9], the feasibility of multicasting video over an infrastructure-based CRN is investigated. The impact of spectrum sensing on multimedia transmission is explored in [13]. Similarly, auction-based schemes are proposed for multimedia streaming in CRs [14] to allocate spectrum in a distributed manner. Yu *et al.* [11] propose application-layer QoS optimization for multimedia transmission over CRNs in which SUs adopt their intraframe refreshing rate based on the sensed channel conditions. The proposed work is a joint source and physical layer solution that does not incorporate the network support for QoS-constrained multimedia delivery. Multimedia transmission over CRNs is also investigated in [12], which uses priority queues to model both the PU traffic and the SU traffic. In [15], the spectrum is segmented according to the multimedia signal samples, and transmission is carried out by using sample division multiplexing. These studies focus on the best channel selection approach in terms of higher capacity and lower interference that does not necessarily mean to support multimedia on the candidate network. Hence, the existing cross-layer solutions do not consider the route selection, prioritized medium access, and yet formidable source admission control to avoid degradation of the current traffic.

A cluster-based QoS routing for multimedia delivery is proposed in [18] that considers multichannels in WSNs. It assumes that the nodes are heterogeneous in which cluster heads are equipped with multiple interfaces and thus able to transmit simultaneously on all the channels. In practice, an such assumption is not realistic since the sensor nodes are assumed low cost and small devices. Moreover, the approach is not pertinent to CRs since the presence of PUs is ignored in dynamic spectrum access. A QoS routing protocol is also proposed in [19] that integrates the routing, channel selection, and transmission power control aiming to provide higher throughput and constrained end-to-end delay. The protocol cannot provide performance guarantees to the current flows since the shortest path routing does not adhere to the sustained QoS routing as the number of flows grows.

Zhou *et al.* [27] propose a distributed scheduling algorithm (DMDS) for video streaming over multichannel multiradio devices in wireless networks, aiming to preserve the QoS for each individual stream. DMDS does not employ a CR for dynamic spectrum access and assumes that the set of given channels are always available to the nodes, i.e., fixed channels. Second, the nodes employ a single radio in this paper, whereas DMDS assumes multiple interfaces on a single node and schedules them accordingly. In contrast, this paper implements dynamic spectrum utilization, which is achieved by CR through dynamic spectrum management functions. Moreover, a single radio device will be cheap and energy efficient for low-cost and low-power multimedia devices in sensor networks. Third, the routing protocol in DMDS does not incorporate the energy metric in its routing decision and is therefore unsuitable for low-power devices.

Hence, efficient routing pertinent to multimedia application in CRSNs is not yet explored, and this is the first study that considers the resource constraint, along with the dynamic

spectrum access, for multimedia routing in CRSNs. The contributions of SCEEM are threefold. First, it isolates the time and frequency variability of the spectrum for smooth operations of multimedia delivery, i.e., it schedules the channels on the order of longer availability for transmission. Second, it preserves the QoS requirements of each source hop-by-hop by adapting the TDMA frame in a cluster and slot allocation to each source by the cluster head. Third, it achieves energy efficiency through distributed clustering and ensures the QoS at each intermediate cluster rather than end-to-end control at the transport layer.

III. Network Model

We assume that there are N SUs deployed in the network with their initial transmission range of r m, which are deployed in the field of $\mathcal{A}$ m^2 area. Node density ρ is then obtained by $N/\mathcal{A}$. Moreover, nodes are equipped with a single interface module that switches among C traffic channels accessed opportunistically and a predefined common control channel (CC). In addition to SUs, there also exist M PUs, which can appear on C channels at any instant with the mean utilization of $\tau_{\rm on}$ s and mean silent period of $\tau_{\rm off}$ s. We also assume that the channels are not saturated by the PUs such that $M\tau_{\rm on} < C(\tau_{\rm on} + \tau_{\rm off})$ reasonably to concede for SU transmission.

We also assume nonpreemptive SU transmission since the wireless transceiver either operates in transmission mode or reception. That is, once the SU transmission has commenced, it completes its current frame transmission before releasing the channel. Thus, it might cause interference with the PU or delay its transmission. When the SU observes the spectrum to detect the PU transmission S_t, the received signal $S_r(t)$ takes the following form [31]:

$$S_r^s(t) = \begin{cases} n(t), & \text{if } H_0 \\ n(t) + S_t(t), & \text{if } H_1 \end{cases}$$

where H_0 represents the hypothesis corresponding to the PU idle state, and H_1 represents the hypothesis corresponding to the transmission state. $n(t)$ is zero-mean additive white Gaussian noise (AWGN). We assume that the energy detection is applied in a nonfading environment for spectrum sensing. The probability of detection P_d and that of false alarm P_f are given as follows [31]:

$$P_d = \Pr\{Y > \epsilon | H_1\}$$
$$P_f = \Pr\{Y > \epsilon | H_0\}$$

where Y is the decision statistic obtained from the energy detection algorithm, and ϵ is the decision threshold. A Low P_d would result in missing the presence of the PUs with high probability, which in turn increases the interference to the PU. On the other hand, a high P_f would result in low spectrum utilization since false alarms increase the number of missed opportunities. Thus, we use a binary variable x_c to represent the availability of a channel c. For node i sensing channel c, $x_c^i = 1$ if $P_d < 0.1$ to represent the absence of PUs on channel c; otherwise, it takes 0.

SU nodes are configured as single-hop distributed clusters in which a node is elected as a cluster head among a group of neighbors, whereas the rest of the neighbors are the members of clusters. A member node transmits data packets to clusters that decide the forwarding path. Thus, the transmission is controlled by the distributed cluster heads. Moreover, each node implements both the TDMA and CSMA medium access control (MAC) protocol operating at different time instants, i.e., at any time t, a node either runs TDMA or CSMA.

We assume that the source employs adaptive video coding H.264/MPEG4 [25] that transmits data as a sequence of frames, which are mainly of three types: intraframe or spatially correlated frame (I-frame), interframe predictive or temporally correlated frame (P-frame), and bidirectionally predictive frame (B-frame). In a particular video sequence, the frames are organized to form a group of picture (GOP) of size $\mathcal{G}$ that consists of an I-frame followed by F_P number of P-frames and then F_B number of B-frames. Assume that these frames are generated at the rate of $\lambda(t)$ at time instant t with tolerable end-to-end latency of $\tau_{\rm e2e}$. Furthermore, the size of an I-frame is assumed twice the size of a P-frame and four times the size of a B-frame [25], approximately. However, we assume that P- and B-frames can be transmitted in one slot, whereas an I-frame would require two slots for transmission.

IV. Spectrum-Aware Cluster-Based Energy-Efficient Multimedia Routing

Here, we present the design of the SCEEM routing protocol for CRSNs. Cluster-based data routing is the potential distributed approach that achieves a suboptimal solution for end-to-end QoS support. In SCEEM, SU nodes form a group or a cluster, which have a higher number of commonly available idle channels or higher spectrum rank.[1] A cluster head is elected among the group that has the highest spectrum energy rank. Cluster heads employ a hybrid TDMA and CSMA approach for medium access such that the TDMA approach is used within a cluster, whereas intercluster medium access is based on the CSMA technique. Moreover, we evaluate the optimal number of clusters to achieve the objective of minimum distortion of multimedia sources, as described in Section IV-B. To maintain QoS, source nodes implement rate-adaptive coding and adopt their data rate according to the slot allocation by the cluster heads for graceful degradation and to avoid retransmission. In the following, we first discuss the clustering algorithm with routing and then evaluate the optimal number of clusters for minimum distortion.

A. Spectrum-Aware Node Clustering

Node clustering is performed to provide distributed control over data transmission. Lacking any traffic control on the multimedia sources can quickly hamper the performance of nodes if the traffic exceeds the capacity of forwarding links and routes. In a cluster-based configuration, a cluster head controls the transmission of nodes participating as members and therefore avoids awkward performance degradation with an increased

[1]The spectrum rank of a node represents the mean transmission opportunity measured by the node on a given set of channels or spectrum.

number of traffic sources. A TDMA approach employed by the cluster head exhibits respectable performance for video sources, if not guaranteed, in a distributed fashion without requiring network-wide synchronization. The key challenge in CRSNs is to support the spectrum cognition with sustained QoS. Thus, the primary criterion in forming clusters is the spectrum awareness of nodes apart from the energy.

In SCEEM, the clustering phase precedes with spectrum sensing on a potential list of bands for a fixed sensing period. After gathering spectrum measurements, the information sharing phase begins in which each node shares the necessary information with its neighbors that is used in selection of a cluster head. This is achieved by a broadcast *Info* message on common CC that contains the channel vacancy indicator, and statistically computed expected vacancy ratio and availability time. Let $\mathbf{v}_i(t)$ be the channel vacancy matrix of node i at time t for C channels in which the binary element $x_c^i(t)$ takes the value of 1 if the channel $c \in C$ is sensed vacant; otherwise, it takes the value of 0. Thus, $\mathbf{v}_i(t) = [x_1^i(t)\ x_2^i(t)\ \cdots\ x_C^i(t)]^T$.

Likewise, $\mathbf{a}_i(t)$ represents the expected channel availability vector for node i, which is a measure of mean available time of each vacant channel and is obtained as $\mathbf{a}_i(t) = [a_1^i(t)\ a_2^i(t)\ \cdots\ a_C^i(t)]^T$. The mean available time of a channel is computed as an exponentially weighted average on past channel statistics [26]. Then, we compute the associated channel availability matrix $\mathbf{A}^{ij}$ of two nodes i and j that permits them to access the channels between them as $\mathbf{A}^{ij}(t) = (\mathbf{v}_i \mathbf{v}_j) \times \min\{\mathbf{a}_i, \mathbf{a}_j\}$, where min is an element-wise minimum operation of two matrices. Node i computes the relative spectrum availability rank Υ for neighboring node j as $\Upsilon^{ij}(t) = (1/C)(\mathbf{1} \cdot \mathbf{A}^{ij}(t))$, where $\mathbf{1} = \{1_1, 1_2, \ldots, 1_C\}^T$ is a binary matrix such that $1_i = 1$. Thus, a node computes the associated rank for each of its neighbor and determines its cumulative spectrum energy rank as

$$\mathbf{\Upsilon}_i(t) = \sum_{j \in \mathcal{N}_i} \Upsilon^{ij}(t) \frac{e_i}{\max_{\forall k \in \mathcal{N}_i}\{e_k\}} \tag{1}$$

where $\mathcal{N}_i$ represents the set of neighbors of node i.

1) Cluster-Head Selection: The cumulative spectrum energy rank computed earlier is used as the criterion for the cluster-head selection, which is described as follows.

- Every node constructs matrices $\mathbf{v}$ and $\mathbf{a}$ in the spectrum sensing phase, as described earlier.
- Nodes report the spectrum information and their residual energy in the broadcast *Info* message during cluster formation phase.
- A node computes its cumulative spectrum energy rank $\mathbf{\Upsilon}_i(t)$ with each of its neighbors using (1) and also computes the rank $\mathbf{\Upsilon}_k(t)$ for all of its neighbors $k \in \mathcal{N}_i$.
- It compares its rank against all the neighbors' ranks, and if it is found to be among the three highest ranks, it then becomes a potential cluster head.
- Node i then runs a random CH timer between $\mathrm{CW}_{\min}$ and $(\mathrm{CW}_{\min} + (\mathrm{CW}_{\min}/2)^s)$ slots and waits for the expiry of the timer to pronounce itself as a cluster head. Here, s is its order among the locally three highest ranked nodes.
- If it receives a cluster-head announcement message from one of its neighbors before its CH timer expires, then it cancels its timer and joins the cluster as a member. However, if it does not receive any CH message during the CH timer period, then it broadcasts the CH message notifying the neighbors to participate as members.
- If a node receives multiple CH messages from its different neighbors, then it joins the cluster k for which it computes the highest rank $\mathbf{\Upsilon}_k(t)$.
- All the nodes synchronize their timers with their cluster heads upon the arrival of the CH message; hence, the data transmission phase begins.

Note that member synchronization may be slightly erroneous due to the propagation time computation. However, sensor nodes usually transmit at a short range with a maximum of 100 m that may cause the worst inaccuracy of 3 μs, which is compensated for by leaving a transmission gap of a contention slot (10 μs) at the beginning of each transmission slot. After the clusters are formed, channel selection and scheduling is performed, which is an indispensable operation for spectrum and energy efficiency. Thereafter, cluster heads initiate route establishment, as described in Section IV-D, and data routing takes place in the cycle of transmission rounds. The transmission round $\mathcal{T}$ is composed of the random access period of maximum length T_r and the TDMA frame of variable length T_t, such that $\mathcal{T} = T_r + T_t$.

2) Channel Selection and Scheduling: The channel scheduling algorithm is run by the cluster head to schedule the use of channels over the TDMA frame for the members acquiring time slots. Time slots are allocated in the ascending order of hop delay budget reported by the members in their slot request beacon. We define the expected availability ratio (EAR) $y_i^c(t)$ for determining the average PU presence and deducing the spectrum sensing outcome for channel c by sensor node i. The EAR vector $\mathbf{y}_i(t)$ for sensor i at time t is obtained as

$$\mathbf{y}_i(t) = (1 - \alpha)\mathbf{a}_i(t) + \alpha \cdot \mathbf{y}_i(t-1) \tag{2}$$

where α is the forgetting factor that decides the contribution of previous states to the current state. The cluster head sorts the vector in the descending order of EAR and assigns the channel c for which $x_c^i = 1$ and has the highest value in the vector. Then, it schedules them along with the slot in its TDMA schedule. However, if there is no channel with $x_c^i = 1$ for a node i, i.e., no channel is detected vacant common to the cluster head and member, then it selects the one with the highest EAR value subject to the threshold $y_i^c(t) \geq \mathrm{EAR}_{\mathrm{th}}$. The value of threshold $\mathrm{EAR}_{\mathrm{th}}$ is set corresponding to the TDMA frame.

B. Optimal Clustering

Let K be the number of clusters formed in the network. In cluster-based configuration, a large number of clusters causes the establishment of long routes that intuitively incur high delay. On the other hand, a small number of clusters, due to their large size, leads to higher sharing of cluster bandwidth among the members, resulting in lesser share of bandwidth. Note that the size of a single-hop cluster is controlled through

the transmission radius of a node and henceforth controls the utilization of bandwidth and latency. Thus, we determine the optimal number of clusters K^* that minimizes the distortion of SU video sources.

We also assume a circular deployment field with the sink at the center of the circle of radius R and the hexagonal architecture for the neighborhood clusters with the initial radius r. We also assume that the field is divided into the concentric rings centered at the sink, whose thickness is $2r$ m, i.e., cluster coverage diameter. In this setting, a total of $\Re = (R/2r)$ rings are formed, giving the maximum cluster hopping to the sink. The average number of upstream node routing through ring i is computed in [30] as $(R^2 - (i \times 2r)^2/(2r)^2(2i-1))$. Hence, the expected number of upstream clusters $\kappa_{\rm up}$ in the outer rings are obtained as

$$E[\kappa_{\rm up}] = \frac{1}{\Re}\sum_{i=1}^{\Re}\frac{R^2-(i\times 2r)^2}{(2r)^2(2i-1)}. \tag{3}$$

For multimedia applications, the late arrived packets are also assumed to be lost apart from the losses due to the transmission failures or network congestion. Generally, distortion $\mathcal{D}$ is a function of packet losses $\mathcal{L}$ and GOP size $\mathcal{G}$ [24] given as

$$\mathcal{D}(\mathcal{G},\,\mathcal{L}) = \sigma_{u_o}^2\,\mathcal{L}\sum_{i=1}^{\mathcal{G}-1}\frac{1-\beta_i}{1+\varphi_i} \tag{4}$$

where $\sigma_{u_o}^2$ is a constant value that describes the video decoder sensitivity to an increase in error rate. If the decoder implements error concealment techniques, then the value is kept correspondingly low. β and φ are two model parameters, where $\beta = 1/(\mathcal{G}-1)$, and φ shows the efficiency of a loop filter for removing error whose value can be obtained from some empirical results, as discussed in [24].

Let δ be the slot period set corresponding to the transmission time of a P-frame. Whereas, the size of I-frame is twice the P-frame and would acquire two time slots. If a source is emitting frames at the rate of λ, then it occupies $\lambda(\mathcal{G}+1/\mathcal{G})\times\mathcal{T}$ time slots in a transmission round $\mathcal{T}$. Similarly, if the average number of nodes in a cluster are N/K under the uniform deployment assumption, then the TDMA frame of a transmission round must contain at least $(N\lambda(\mathcal{G}+1)/K\mathcal{G})\mathcal{T}$ slots. However, a cluster also provides routing path to its upstream clusters, and it also spares the time slots in a TDMA frame for upstream clusters, yielding the TDMA frame size n_t as

$$n_t = E[\kappa_{\rm up}]\frac{2N\lambda(\mathcal{G}+1)}{K\mathcal{G}}\mathcal{T}. \tag{5}$$

In practice, the average number of slots q that a source can acquire in a second can be obtained by $(1/n_t\delta)\xi\mathcal{T}\eta$, where ξ is the fraction of transmission round utilized in random access for request propagation. Here, η is the efficiency of a cluster head running TDMA concurrently with the CSMA, as described in Section IV-F. Now, if the slot acquisition rate is lower than the frame emission rate, i.e., $q<\lambda$, then the source suffers frame losses due to insufficient capacity at the cluster head. Hence, the frame loss probability is computed as $(\mathcal{L} = 1-(q/\lambda) - \phi E[\kappa_h])$, where ϕ is the clustering schedule conflict probability in TDMA given by (12). $E[\kappa_h]$ is the expected number of clusters in the routing path computed as $\Re e^{-(2N\delta(G+1)/\tau_{\rm e2e}G)}$. Thus, (4) yields

$$\mathcal{D}(\mathcal{L},\,\mathcal{G}) = G\left(1-\frac{q}{\lambda}-\phi E[\kappa_h]\right) \tag{6}$$

where $G = \sigma_{u_o}^2\sum_{i=1}^{\mathcal{G}-1}((1-\beta_i)/(1+\varphi_i))$. By substituting q in (6) and using (5), the total distortion of N nodes with K clusters is

$$\mathcal{D}_{\mathcal{N}}(\mathcal{L},\,\mathcal{G},\,K) = N\times G\left(1-\frac{\mathcal{G}\eta\xi K}{2E[\kappa_{\rm up}]N(\mathcal{G}+1)\delta\lambda^2}-\frac{\delta E[\kappa_h]}{\mathcal{T}E[C_K]}\right). \tag{7}$$

In the cluster-based configuration, the number of clusters along the field radius R representing the maximum clusters hopping can be computed by $(\sqrt{K}/2)$. Therefore, the delay budget for each cluster will be obtained as $(2\tau_{\rm e2e}/\sqrt{K})$ for the end-to-end deadline $\tau_{\rm e2e}$ of multimedia application. Hence, restricting the transmission round $\mathcal{T}$ in which each source acquires one time slot for its data transmission to the delay budget of a cluster will meet the end-to-end deadline. Substituting the value of $\mathcal{T}$ in (7) and simplifying it, we have

$$\mathcal{D}_{\mathcal{N}}(\mathcal{L},\mathcal{G},K) = G\left(N-\frac{\mathcal{G}\eta\xi K}{2E[\kappa_{\rm up}](\mathcal{G}+1)\delta\lambda^2}-\frac{N\delta E[\kappa_h]\sqrt{K}}{2\tau_{\rm e2e}E[C_K]}\right). \tag{8}$$

Now, if the distortion function in (8) is differentiable and convex, then the local minimum loss causing distortion is achieved as a global minimum. It is analyzed that $(\partial^2\mathcal{D}_{\mathcal{N}}(\mathcal{L},\,\mathcal{G},\,K)/\partial^2 K) > 0$. Hence, differentiating (8) with respect to K and equating it to 0, we achieve the optimal value K^* as follows:

$$\frac{\partial\mathcal{D}_{\mathcal{N}}(\mathcal{L},\,\mathcal{G},\,K)}{\partial K} = -G\left(\frac{\mathcal{G}\eta\xi}{2E[\kappa_{\rm up}](\mathcal{G}+1)\delta\lambda^2}+\frac{N\delta E[\kappa_h]}{4\tau_{\rm e2e}E[C_K]\sqrt{K}}\right) = 0. \tag{9}$$

Simplifying it for K^*, it yields

$$K^* = \left(\frac{NE[\kappa_{\rm up}](\mathcal{G}+1)\delta^2\lambda^2E[\kappa_h]}{2\mathcal{G}\eta\xi\tau_{\rm e2e}E[C_K]}\right)^2. \tag{10}$$

The value of K^* depends on various parameters and therefore can be adopted by setting them appropriately. The most important parameters are the number of SUs N, GOP size $\mathcal{G}$, and end-to-end deadline $(\tau_{\rm e2e})$. Fig. 1 shows the optimal number of clusters for varying the number of nodes at different values of $\tau_{\rm e2e}$. Thus, such adaptive clustering provides flexibility to tune the network configuration according to the performance requirements. Note that once the optimal clusters are obtained, the transmission radius r of nodes is set according to K^*. For instance, r can be computed by $(R/\sqrt{K^*})$ for uniform node deployment given that it does not exceed the interference threshold of the PUs.

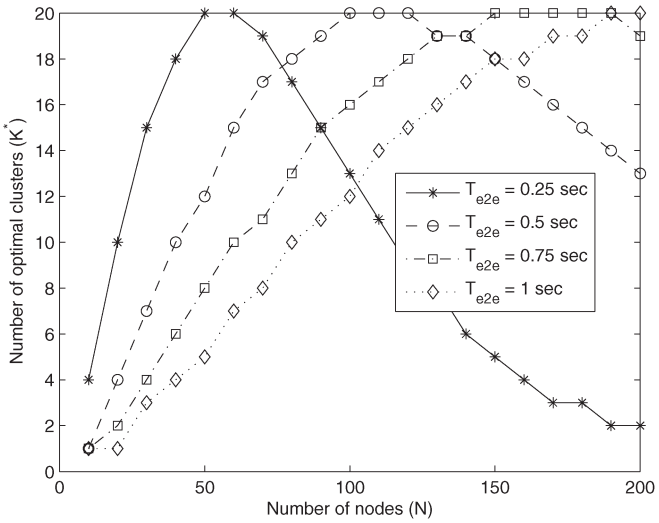

Fig. 1. K^* for different values of (τ_{e2e}) and $\mathcal{G} = 8$.

C. Upper Bound on K

The upper bound on K (K_U) is inferred from the interference threshold on the PU transmission. The SINR value at the PU in the fading channel environment is

$$\gamma = \frac{P^{\mathrm{PU}} G^{\mathrm{PU}}}{\eta^{\mathrm{PU}} + \sum_{i=1}^{M} P_i^{\mathrm{PU}} G_i^{\mathrm{PU}}}$$

where η_p is the white Gaussian noise power at the PU. PUs define an SINR threshold value $\gamma_{\mathrm{th}}^{\mathrm{PU}}$ for successful transmission such that $\gamma_{\mathrm{th}}^{\mathrm{PU}} \leq \gamma$, which yields

$$\gamma_{\mathrm{th}}^{\mathrm{PU}} \leq \frac{P^{\mathrm{PU}} G^{\mathrm{PU}}}{\eta^{\mathrm{PU}} + \sum_{i=1}^{M} P_i^{\mathrm{SU}} G_i^{\mathrm{SU}}}.$$

We assume that all the SUs use homogeneous transmission power and have short-range transmission. Therefore, the interference from all the SUs can be perceived similar with some deviation σ_p^{SU} due to different path loss and shadowing effects. Therefore, the above inequality can be written as

$$\gamma_{\mathrm{th}}^{\mathrm{PU}} \leq \frac{P^{\mathrm{SU}} G^{\mathrm{SU}}}{\eta^{\mathrm{PU}} + \sigma_p^{\mathrm{SU}} M P^{\mathrm{SU}} G^{\mathrm{SU}}}.$$

Since TDMA is employed for intracluster medium access; therefore, only a single node is scheduled to transmit in a given time slot. Intuitively, a K number of SUs corresponding to the number of clusters might be actively transmitting to interfere with the PU transmission. Moreover, if we assume that a cluster schedules at least $C_{\min}$ channels along with the time slot allocation in a round, it yields

$$\gamma_{\mathrm{th}}^{\mathrm{PU}} \leq \frac{P^{\mathrm{SU}} G^{\mathrm{SU}}}{\eta^{\mathrm{PU}} + \sigma_p^{\mathrm{SU}} K / C_{\min} P^{\mathrm{SU}} G^{\mathrm{SU}}}.$$

Note that, if the number of clusters exceeds the value of K, then the interference will increase beyond the limit. Thus, it serves as the upper bound on K as

$$K_U = \frac{C_{\min}\left(P^{\mathrm{SU}} G^{\mathrm{SU}} / \gamma_{\mathrm{th}}^{\mathrm{PU}} - \eta^{\mathrm{PU}}\right)}{\sigma_p^{\mathrm{SU}} P^{\mathrm{SU}} G^{\mathrm{SU}}}. \tag{11}$$

Intuitively, a higher value of K causes more interference to the PU transmission, whereas a smaller K value results in larger cluster size that reduces the bandwidth share of members.

D. Routing

Routing in SCEEM is performed in proactive fashion because only the cluster heads are involved in a route setup, where $K \ll N$, which significantly reduces the routing overhead. After the cluster formation, the routing algorithm runs as follows:

Step 1: Cluster head broadcasts the route request (CH-RREQ) message on CC. Member nodes receive the request and broadcast it further after waiting for the random backoff time. If member node m_j^u overhears CH-RREQ transmitted by another member m_i^u of the same cluster k_u, then it cancels its backoff timer and ignores the message.

Step 2: Nodes of different cluster k_v, receiving the CH-RREQ on the CC channel, run a short backoff random timer, and one of the members m_j^v randomly broadcasts the CH-RREP message if the route is found in its cache. Otherwise, it forwards the CH-RREQ message to its cluster head after waiting for a long backoff time during the random access period of a transmission round. If k_v keeps the route to the sink, then it broadcasts the CH-RREP message containing the number of cluster heads on the path. All the members of k_v cache the route reply information in random access mode, and only m_j^v broadcasts the CH-RREP message. If k_v does not contain route information, then it also forwards the CH-RREQ message, as described in *Step 1*.

Step 3: All the members of the k_u receiving the CH-RREP message from m_j^v cache the route information, and only m_i^u forwards the CH-RREP message to the cluster head k_u.

Step 4: Once the route is found, the cluster head announces the request propagation phase that operates in random access mode on the CC. Member nodes transmit the data request message (M-DREQ) containing the required number of slots along with the type of video frames and also the cached routing information, if it exists, learned in the route establishment phase.

Step 5: If the data request message does not contain route information or the nodes' learned route is not the preferred route, then it is assumed that such nodes are farther from the forwarding cluster and their data are passed through the cluster head itself by allocating TDMA slots. Otherwise, the cluster head does not allocate slots in its TDMA frame, and such nodes are allowed to directly transmit through the forwarding cluster following intercluster routing.

Step 6: At the end of request propagation period, the cluster head prepares its TDMA and spectrum schedule, and broadcasts the H-DSCH message on CC. Member nodes receiving this message synchronize with the cluster head and the TDMA frame commences. Thereafter, every node transmits in its specified time slot on a given traffic channel among the list of C channels dictated by the cluster head.

Hence, routing is controlled by the cluster heads, which is performed in a number of transmission rounds during the clustering period. In the random access period, nodes use the carrier sensing access technique to transmit their data request

beacons to their cluster heads. The random access period terminates when either its maximum duration is reached or when no request is received by the cluster head for a period set corresponding to maximum contention window size. To meet the deadline τ_{e2e}, the cluster head limits its transmission round to the delay budget computed using τ_{e2e} and the number of clusters on the path. Clusters are reformed at the end of the clustering period, which is determined based on how long the spectrum information remains accurate by the cluster head such that transmission is made successful on the vacant spectrum bands, as well as the energy depletion rate of the cluster head. In the TDMA frame used for intracluster transmission, the cluster head allocates a time slot δ to each member requesting for transmission, whereas it retains each alternative time slot for immediate forwarding.

To avoid jitter, the cluster head maintains the order of slot allocation in each transmission round, where the order in the first round is decided based on the hop delay budget and type of frames contained in the M-DREQ message with an I-frame given the highest priority. Notably, a node follows the TDMA schedule, i.e., synchronizes with the cluster head, only when either it is the allocated slot for transmission or it is scheduled as a receiver for data routing. Otherwise, it remains tuned to the common CC and operates in CSMA mode. When a gateway node n_i^u receives data in the TDMA frame from its cluster head k_u for intercluster routing, it switches to common CC and operates in CSMA mode. Since nodes only operate in TDMA mode either for transmission or reception, it is highly likely that n_i^u finds a member node n_j^v of downstream cluster k_v in CSMA mode. Thus, n_i^u sends the channel contention beacon (M-CRTS) on common CC containing the list of its vacant channels. One of the downstream members n_j^v having a common vacant traffic channel replies (M-CCTS) back to n_i^u, notifying its decision on the usage of traffic channel c and, thereafter, tunes to channel c. n_i^u receives the message and also tunes to the notified traffic channel c. It then transmits the data packet to n_j^v and waits for the acknowledgment (ACK). If the data packet is successfully received by n_j^v, it sends an ACK and switches back to the common CC. If n_i^u receives the ACK, it releases the packet from its buffer and also switches to the common CC. However, if it does not receive ACK, then it repeats the channel contention and retransmits the packet.

A node can run in CSMA mode, whereas a TDMA frame of its cluster is in progress. However, if there is a single gateway node, then it needs to synch with the cluster for every alternative slot to receive the forwarding packet. In this case, it cannot run in both TDMA and CSMA modes. On the other hand, if there are at least two gateway nodes, then a gateway node needs to synch with the cluster head after three time slots, and it is highly likely that it completes its CSMA transmission within three time slots.The higher the number of gateway nodes, the more concurrently the TDMA and CSMA operate, and eventually, the lesser the delay that is incurred.

E. Energy Efficiency

Energy efficiency in SCEEM is achieved in two ways: energy and spectrum-aware clustering and avoiding overhearing in data transmission. The rank computed in (1), used for cluster-head selection, includes the energy of the node and considers the ratio of its residual energy with the maximum energy of the neighboring nodes. The higher the energy of a node is relative to its neighbors, the larger the rank is, and eventually, the higher the possibility of becoming a cluster head. After the cluster formation, the cluster head establishes the routing path for all of its members and performs forwarding. Thus, more routing operations are performed by the higher energy node, i.e., the cluster head, that results in energy efficiency. Clusters are reformed periodically or when the cluster-head residual energy becomes lower than the members to balance the energy consumption. Furthermore, nodes switch to common CC if they are not a transmitter or a receiver of a slot in the TDMA schedule. In this way, they greatly avoid consuming energy in overhearing during the data transmission.

F. Performance Analysis

The performance of cluster-based routing greatly depends on the size of a cluster. Once the optimal cluster size is determined, the size is estimated by equally distributing the nodes to each cluster due to uniform distribution. Thus, for a given size of the cluster $Q = (N/K^*)$, the performance is derived as how efficiently or concurrently TDMA and CSMA operates in data routing. Since the TDMA schedule is defined locally in a cluster, it might conflict with the schedule of neighboring clusters. Therefore, the probability that a packet is transmitted successfully in a given time slot depends on the vulnerable TDMA frame period, the number of clusters causing conflict, and the number of idle channels C_K that can be potentially used in the frame schedule. Assuming that all the PUs can affect the transmission of all the SUs, the probability of channel vacancy can be computed by $p_v = 1 - (M\tau_{\mathrm{on}}/(C(\tau_{\mathrm{on}} + \tau_{\mathrm{off}})))$, Thus, the expected number of idle channels in a cluster is

$$E[C_K] = \sum_{c=1}^{C} c\binom{C}{c} p_v^c (1-p_v)^{C-c}.$$

If nodes from the adjacent clusters transmit in the same slot, then they experience collision causing transmission failure. Thus, for a slot period δ in a transmission round $\mathcal{T}$, the probability of interference with a neighboring cluster operating on the same channel is $\delta/\mathcal{T}$. However, for the expected number of channels $E[C_K]$ that the two nearby clusters can operate, the probability reduces to $(\delta/\mathcal{T}E[C_K])$. For simplicity, we assume hexagonal clustering architecture in which a cluster can be interfered by six neighboring clusters. The hexagon shape closely approximates the circle, which is presumably the coverage geometry of wireless transmission in an open field. Therefore, hexagon represents the extreme case of interference by the neighboring clusters, and in turn, the probability of TDMA schedule conflict is higher. The probability that a node suffers schedule conflict with adjacent cluster nodes is obtained as

$$\phi = \left(\frac{\delta}{\mathcal{T}E[C_K]}\right)^6. \tag{12}$$

When a node does not overhear the transmission of its packet by the cluster head in the following slot, the packet is assumed lost due to the conflict and will be retransmitted. Similarly, if the spectrum sensing is performed with certain false alarm probability p_f, then the PU transmission may also interfere with the SU transmission. In both cases, a node may need to wait for the entire transmission round to get the opportunity in the next TDMA frame. Hence, the TDMA scheme yields intracluster packet delay as $\tau_t = (\bar{\mathcal{T}}/(1-(\phi+p_f)))$.

When the gateway members are limited for intercluster routing, they would not be able to run CSMA concurrently and frames will be logged. Cluster heads extend the random access period until the logged packets are routed. Eventually, the T_r period may span over the request propagation in addition to the intercluster routing latency. Recall that a node first negotiates the traffic channel in the CSMA-based technique, as described in Section IV-D, by sending a request on a common CC. The bandwidth of the common channel is presumably limited that constrains the access to traffic channels. The larger the number of contending gateway nodes, the higher the probability of collision. The possible gateway nodes Q_{gw} of a cluster can be determined by the node density as $\rho \times A_F$. A_F is the forwarding segment of a cluster-head coverage at minimum routing progress a unit of distance. By using trigonometry and simplification, A_F is computed as

$$A_F = 2\arcsin\left(\sin\left(\frac{\pi}{4}\right)\frac{\sqrt{r^2-a^2}}{r}\right)r^2 - a\sqrt{r^2-a^2}. \quad (13)$$

The probability p_s that a gateway node successfully transmits on the CC is obtained as

$$p_s = Q_{\mathrm{gw}}\frac{1}{\mathrm{CW}}\sum_{w=1}^{\mathrm{CW}}\left(\frac{\mathrm{CW}-w}{\mathrm{CW}}\right)^{Q_{\mathrm{gw}-1}}.$$

Similarly, the backoff time that a node defers its transmission in a CSMA protocol is computed by

$$T_{\mathrm{bo}} = \sum_{j=1}^{J}(1-p_s)\frac{\min(2^j\mathrm{CW}_{\min},\,\mathrm{CW})-1}{2}\delta.$$

As a result, the rate of possible channel negotiation requests on the CC is determined as

$$\mu_n = (1-O_n)\frac{T_c}{T_n}\times\frac{B_{\mathrm{cc}}}{S_c} \quad (14)$$

where the total channel negotiation time T_n is $\mathrm{DIFS} + T_{\mathrm{bo}} + 2T_c + \mathrm{SIFS}$, S_c is the size of control frame, B_{cc} is the bandwidth of common CC, and O_n is the overhead time used in negotiation, which is computed by $((\mathrm{DIFS} + T_{\mathrm{bo}} + \mathrm{SIFS})/T_n)$. Hence, the average delay to negotiate the traffic channel using the common CC is $1/\mu_n$.

After negotiating the traffic channel, both the transmitting and receiving nodes switch to the traffic channel c, which is not currently scheduled in the TDMA frames of the clusters of both nodes. On the traffic channel, the transmitter waits for DIFS time and transmits its data frame. The receiving node receives the frame, waits for SIFS time, and sends an ACK to the transmitter. Therefore, the delay incurred on data transmission at a gateway node is $(1/\mu_d) = \mathrm{DIFS} + (S_d/b_c(t)) + \mathrm{SIFS} + (S_c/b_c(t))$ with a data transmission rate of μ_d. With the spectrum false alarm probability p_f, retransmission is provoked that causes increase in the delay accordingly. Thus, yielding intercluster forwarding latency τ_f as

$$\tau_f = \frac{1}{p_f}\left(\frac{1}{\mu_n}+\frac{1}{\mu_d}\right). \quad (15)$$

Since the concurrent execution of TDMA and CSMA brings efficiency to the cluster in terms of lesser delay, we determine the efficiency probability η that CSMA does not cause latency in scheduling the TDMA frame. We assume that CSMA can run in parallel with TDMA if there are at least two gateway members of a cluster used alternatively given that $\tau_f < 3\delta$, as described in Section IV-D. Thus, the probability that the two access techniques run concurrently is computed as

$$\begin{aligned}\eta &= \Pr(\tau_f < 3\delta)\times\Pr(Q_{\mathrm{gw}}\geq 2)\\ &= \Pr(\tau_f<3\delta)\,(1-\Pr(Q_{\mathrm{gw}}=1))\end{aligned} \quad (16)$$

where $\Pr(\tau_f < 3\delta) = 1 - e^{-(\tau_f/3\delta)}$ since τ_f is exponentially distributed over the mean delay 3δ due to the use of CSMA for intercluster routing. The probability of gateways availability is computed as

$$\begin{aligned}\Pr(Q_{\mathrm{gw}}=1) &= \frac{A_F}{\mathcal{A}}\left(1-\frac{A_F}{2\mathcal{A}}\right)^{N-1}\binom{N}{1}\\ &= \frac{N}{\mathcal{A}}A_F\left(1-\frac{A_F}{\mathcal{A}}\right)^{N-1}\\ &= Q_{\mathrm{gw}}\left(1-\frac{A_F}{\mathcal{A}}\right)^{N-1}.\end{aligned} \quad (17)$$

Substituting (17) in (16) and using (15), it yields

$$\eta = \left(1-e^{-\frac{\mu_n+\mu_d}{3\delta p_f\mu_n\mu_d}}\right)\left(1-Q_{\mathrm{gw}}\left(1-\frac{A_F}{\mathcal{A}}\right)^{N-1}\right). \quad (18)$$

Hence, η characterizes the efficiency of cluster-based routing in terms of reducing the delay by employing the hybrid medium access technique. Whereas, the bandwidth for each source is provisioned by the cluster heads through the TDMA schedule.

V. Performance Evaluation

The performance of the SCEEM is evaluated using *ns-2* [32] with rate-adaptive extension [29]. In *ns-2*, SCEEM is implemented as a routing agent. The IEEE 802.11 MAC protocol is customized for CR support; therefore, the modified 802.11cr is used as the CSMA MAC agent in our simulation script. The CRN patch [33] is applied to *ns-2* that enables the support of multiple channels at the physical layer, which are indexed to select a particular channel at any given time instant. We measure the video quality in terms of PSNR, clustering efficiency in terms of delay and energy, and routing performance using end-to-end packet delay, delivery ratio, and jitter in comparison to the existing routing protocol SEARCH [21]. The deployment

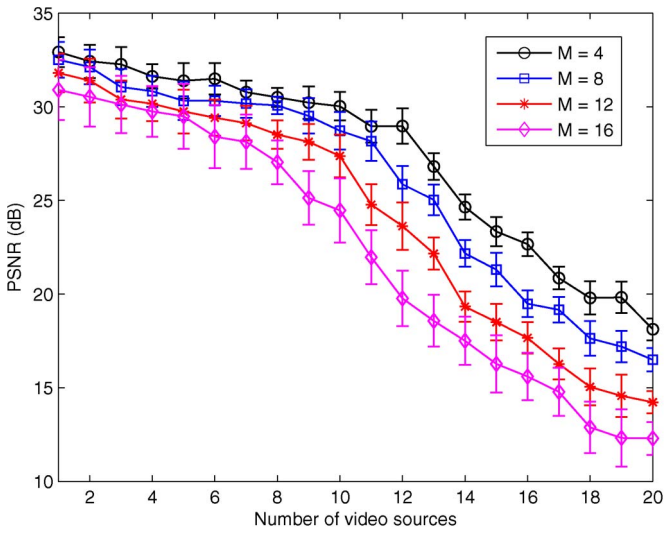

Fig. 2. Average PSNR for different numbers of PUs by varying SU sources at $C = 10$.

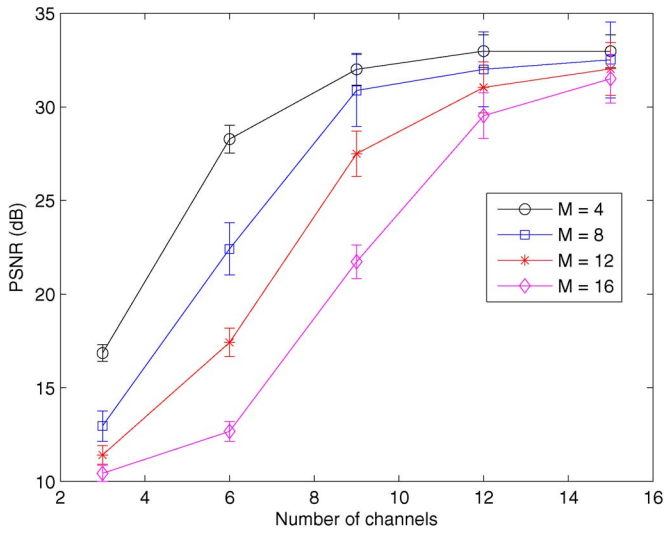

Fig. 3. Average PSNR for different numbers of PUs by varying the number of channels at five SU sources.

field is set to 300×300 m^2 area containing up to 16 PUs and uniformly deployed 100 SUs with *foreman* video delivery. PU traffic is exponentially ON/OFF with $\tau_{\text{off}} = 0.5$ and $\tau_{\text{on}} = 0.5$ s and up to ten channels are used for transmission and PUs appear on these channels randomly. The packet deadline for SU video sources is set to 500 ms. The data slot in TDMA is set to 1200-B transmission period of the link layer rate. The clustering and random access periods are set to 50 ms each, given that the Info and M-DREQ messages are up to 100 B and the cluster size is of 10 nodes approximately.

A. Video Quality

To measure the video quality of SUs in CRSNs, we set up two different scenarios: first, by changing the number of SU sources and, second, by changing the number of channels. Fig. 2 shows the mean PSNR by increasing the number of sources from 1 to 20 at different number of PUs. It can be observed that the PSNR value does not decay significantly up to 12 SUs at lesser number of PUs, i.e., $M = 4$, that can be rated *Good* (PSNR $>= 30$). However, the same level of quality is achieved only for six SUs at $M = 16$. Thus, by increasing the number of PUs by four times, the number of SUs sustaining the same PSNR are decreased only by half. This is achieved because there is enough transmission time available for SUs and the clustering approach efficiently utilizes that by avoiding every node to coordinate for traffic channel. However, by increasing SU sources further, the PSNR value drops sharply, which is because of rate-adaptive sources that change their quantization scale to decrease the data rate when the data requests in a TDMA frame cannot be fulfilled by cluster heads, thus causing a lower PSNR value. Intuitively, by increasing SU sources from 1 to 10 at $M = 4$, the PSNR is decreased by only 2 dB because the time and channel allocation by cluster heads ensure the continuous availability of transmission. On the other hand, it decreases 13 dB by increasing SUs from 10 to 20, which shows insufficient transmission opportunity for the large number of video sources.

In the second scenario, the PSNR value is measured for a fixed number of SU sources but the number of channels is varied to investigate the impact of available spectrum band, as shown in Fig. 3. It can be observed that the PSNR value is very low at small number of channels but increases exponentially by increasing the number of channels. At lower PUs ($M = 4$), the PSNR value reaches close to the threshold of 30 dB at only $C = 6$, whereas it requires nine channels, only 50% higher, to reach the threshold at twice the number of PUs ($M = 8$). This implies that, as the transmission opportunity is provided to SUs, SCEEM quickly adopts and utilizes it efficiently. Moreover, as the video quality converges to its maximum value, the increase in the channel number does not improve it further, showing the excessive capacity for SUs. However, this limit is reached at a smaller number of channels with a lower value of M but requires a larger number channels for higher M. Hence, by adding three channels into the channels list, the PSNR is improved to 9 dB before it converges to its maximum value.

B. Clustering Efficiency

The optimal clustering is verified through simulation experiments in terms of end-to-end delay and energy consumption. The number of clusters in a network are controlled by changing the transmission power accordingly. For the given setup of 100 SUs, GOP size of 12 ($\mathcal{G} = 12$), and three sources, the optimal number of clusters computed are 19, as shown in Fig. 1. However, as the traffic increases beyond the capacity of optimal clusters (for 6 video sources), the performance drops, which should be controlled either by providing a greater number of channels or restricting the number of active SUs. Fig. 4(a) shows that the delay increases with the increase in number of clusters due to a large number of hops. However, the limit of 400 ms can be preserved up to 22 clusters. Similarly, the maximum node energy consumption is lower at about 20 clusters, as shown in Fig. 4(b), which cannot be further saved by increasing the number of clusters. Thus, the lower energy consumption is achieved at 20 clusters, and the end-to-end

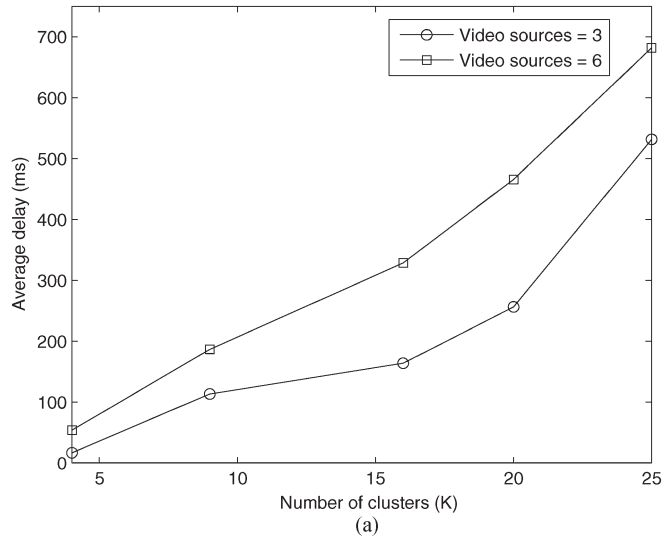

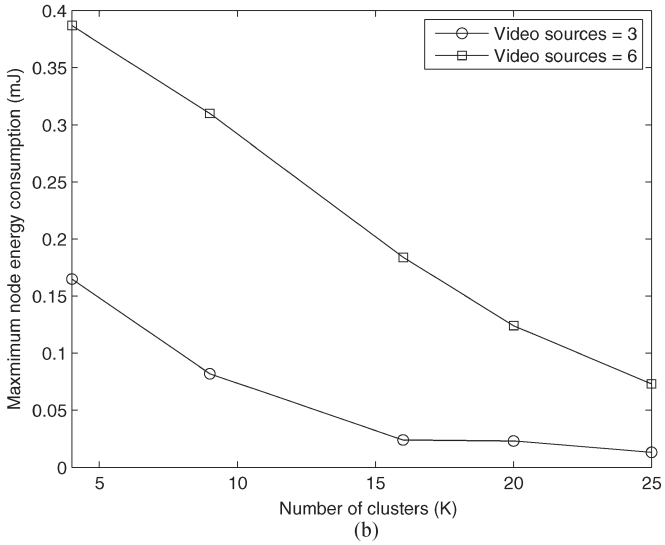

Fig. 4. Performance of the routing protocol by varying the number of clusters K, $M = 10$, and $C = 10$. (a) Average delay of video sources at different numbers of clusters. (b) Maximum energy consumption of an SU node at different numbers of clusters.

delay is below the deadline of 400 ms at $K = 20$. Hence, it reveals that the optimal number of clusters in SCEEM achieves lower energy consumption and meets the packet deadline.

To investigate the efficient utilization of spectrum by the proposed protocol, Fig. 5 demonstrates the channel utilization for SUs and PUs with the interference. It can be clearly seen that, the channels, which are utilized frequently by PUs, are less likely used for SU transmission. This is because the cluster head schedules the transmission of its members over the channels that can remain available over the longer period or the entire TDMA frame of a cluster. It can be observed that channel 9 has the highest SU transmission time, whereas channels 1, 2, and 4 have the lower SU transmission time since they are mostly used by PUs. Hence, the cluster-head selection based on spectrum rank and the transmission scheduling based on channel rank by the cluster head show the given spectrum utilization pattern in Fig. 5. Moreover, the interference of SU with the PU is also below 10% of the PU transmission time.

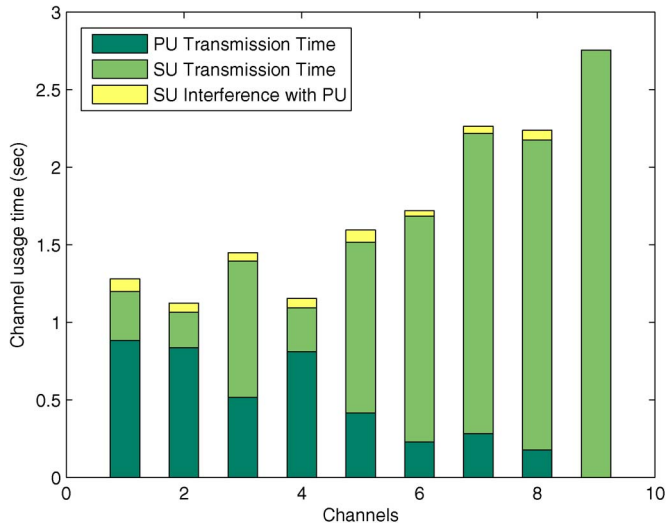

Fig. 5. Channel usage time of PUs and SUs at $C = 10$.

C. Routing Efficiency

The efficiency of routing in SCEEM is investigated for end-to-end packet delay and delivery ratio, which is also compared with the SEARCH protocol proposed for CR ad hoc networks. Here, we consider a scenario that has three active SUs with CBR traffic in addition to the presence of ten PUs. The data rate of SU sources is varied in 100–700 kb/s. Fig. 6(a) reports the comparison of average delay that shows a significantly lower delay in SCEEM, as compared with SEARCH. The delay increases exponentially in SEARCH, whereas this increase is linear in SCEEM. The delay in SCEEM remains almost unchanged up to the load of 300 kb/s since the packet rate is within the limit of TDMA frame size of clusters but increases linearly thereafter due to a higher packet rate exceeding the maximum TDMA frame size in a cluster. In contrast, SEARCH involves every node in route establishment and maintenance that causes significant overhead traffic, therefore increasing the delay at a higher rate. Eventually, the delay in SCEEM is about 250% lower than SEARCH at a 700-kb/s data rate. The hybrid MAC in SCEEM is also compared with the CSMA-only access technique with the SCEEM routing agent. The delay in CSMA is higher and grows exponentially with the increase in the source data rate. The same trend is also observed in the packet delivery ratio shown in Fig. 6(b) that shows approximately 300% times higher delivery ratio in SCEEM. It is important to note that the delay in SEARCH does not increase significantly after the rate is increased above 400 kb/s because the packet delivery ratio is dropped considerably low to 0.3, and this drop results in the lower increase in the delay beyond that rate. Hence, the hybrid access technique in SCEEM performs better than SEARCH in terms of delay and delivery ratio. It is also proven to be an energy-efficient solution as well due to its clustering architecture.

VI. Conclusion

This paper addresses the problem of multimedia routing in CRSN by proposing a cluster-based solution. Clustering

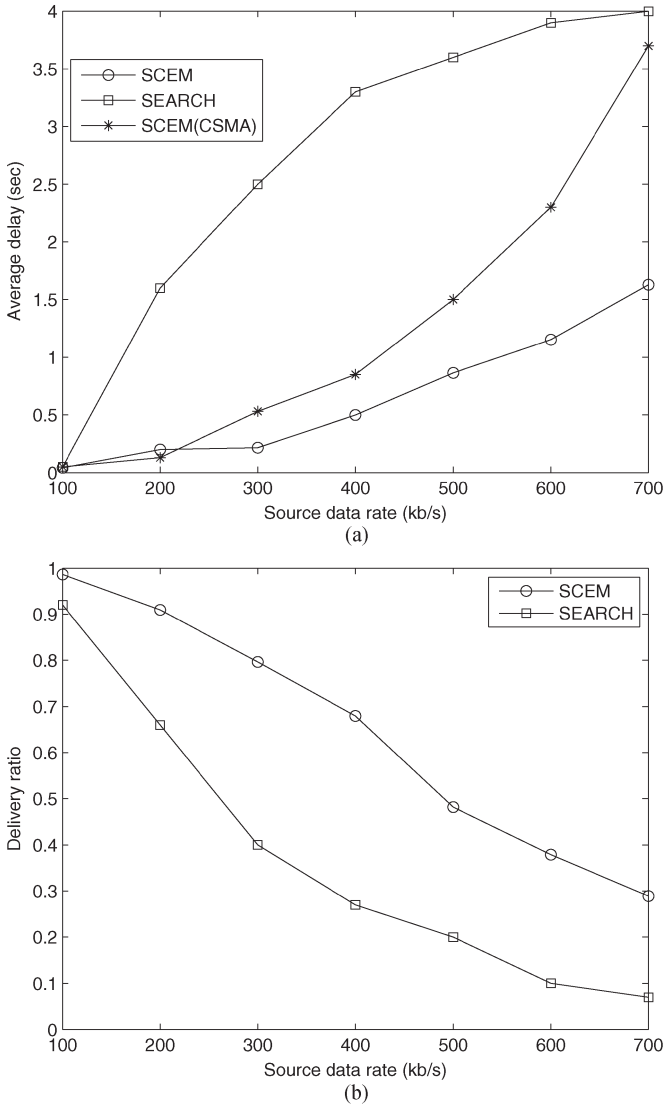

Fig. 6. Performance comparison of the proposed protocol with SEARCH by varying the traffic load. (a) Average delay comparison of SCEEM with SEARCH [21] protocol by varying the traffic load. (b) Delivery ratio comparison of SCEEM with SEARCH [21] protocol by varying the traffic load.

is exploited to manage dynamic spectrum access and QoS routing for multimedia CRSNs. The number of clusters are computed optimally according to the given network scenario and transmission power is adopted to manage the formation of the optimal number of clusters in the network. A spectrum-aware cluster-head selection is made in which channels are clustered using the spectrum sensing results obtained in each round along with the spectrum usage statistics and past experience of cluster heads. Routing in SCEEM is based on hybrid TDMA and CSMA MAC protocol to relay intracluster and intercluster packets, respectively. Performance results reveal that SCEEM achieves higher PSNR for SU video sources through the adaptive data sources and cluster-based transmission control. Moreover, its optimal clustering provides energy-efficient multimedia delivery with the desired QoS support. The routing performance is also compared with the existing routing protocol for CR ad hoc networks, and it incurs three times lesser delay with a higher delivery ratio.

REFERENCES

[1] O. B. Akan, O. B. Karli, and O. Ergul, "Cognitive radio sensor networks," *IEEE Netw.*, vol. 23, no. 4, pp. 34–40, Jul./Aug. 2009.

[2] M. D. Felice, R. D. Mohammady, K. R. Chowdhury, and L. Bononi, "Smart radios for smart vehicles: Cognitive vehicular networks," *IEEE Veh. Technol. Mag.*, vol. 7, no. 2, pp. 26–33, Jun. 2012.

[3] G. A. Shah and O. B. Akan, "Spectrum-aware cluster-based routing for cognitive radio sensor networks," in *Proc. IEEE Commun.*, Jun. 9–13, 2013, pp. 2885–2889.

[4] G. A. Shah, V. C. Gungor, and O. B. Akan, "A cross-layer design for QoS support in cognitive radio sensor networks for smart grid applications," in *Proc. IEEE ICC*, Jun. 2012, pp. 1378–1382.

[5] A. Wilzeck, E. Dimitrov, and A. Tissen, "Applications of cognitive radio systems for industrial wireless automation," in *Proc. 4th ACM CogART*, Oct. 2011, p. 65.

[6] L. Bixio, L. Ciardelli, M. Ottonello, and C. S. Regazzoni, "Distributed cognitive sensor network approach for surveillance applications," in *Proc. IEEE AVSS*, Sep. 2009, pp. 232–237.

[7] N. Ikram, S. Durranii, H. Sajid, and H. Saeed, "A wireless multimedia sensor network based intelligent safety and security system (IS^3)," in *Proc. SENSORCOMM*, Jun. 2009, pp. 388–392.

[8] S. Misra, M. Reisslein, and X. Guoliang, "A survey of multimedia streaming in wireless sensor networks," *IEEE Commun. Surveys Tuts.*, vol. 10, no. 4, pp. 18–39, 4th Qtr., 2008.

[9] H. Donglin, M. Shiwen, Y. T. Hou, and J. H. Reed, "Scalable video multicast in cognitive radio networks," *IEEE J. Sel. Areas Commun.*, vol. 28, no. 3, pp. 334–344, Apr. 2010.

[10] H. Donglin and M. Shiwen, "Streaming scalable videos over multi-hop cognitive radio networks," *IEEE Trans. Wireless Commun.*, vol. 9, no. 11, pp. 3501–3511, Nov. 2010.

[11] F. R. Yu, B. Sun, V. Krishnamurthy, and S. Ali, "Application layer QoS optimization for multimedia transmission over cognitive radio networks," *Wireless Netw.*, vol. 17, no. 2, pp. 371–383, Feb. 2011.

[12] S. Hsien-Po and M. van der Schaar, "Queuing-based dynamic channel selection for heterogeneous multimedia applications over cognitive radio networks," *IEEE Trans. Multimedia*, vol. 10, no. 5, pp. 896–909, Aug. 2008.

[13] X. L. Huang, G. Wang, F. Hu, and S. Kumar, "The impact of spectrum sensing frequency and packet-loading scheme on multimedia transmission over cognitive radio networks," *IEEE Trans. Multimedia*, vol. 13, no. 4, pp. 748–761, Aug. 2011.

[14] Y. Chen, Y. Wu, B. Wang, and K. J. R. Liu, "Spectrum auction games for multimedia streaming over cognitive radio networks," *IEEE Trans. Commun.*, vol. 58, no. 8, pp. 2381–2390, Aug. 2010.

[15] A. Bhattacharya, R. Ghosh, K. Sinha, and B. P. Sinha, "Multimedia communication in cognitive radio networks based on sample division multiplexing," in *Proc. 3rd COMSNETS*, Jan. 2011, pp. 1–8.

[16] A. Al-Fuqaha, B. Khan, A. Rayes, M. Guizani, O. Awwad, and G. B. Brahim, "Opportunistic channel selection strategy for better QoS in cooperative networks with cognitive radio capabilities," *IEEE J. Sel. Areas Commun.*, vol. 26, no. 1, pp. 156–167, Jan. 2008.

[17] T. Liu and W. Liao, "Interference-aware QoS routing for multi-rate multi-radio multi-channel IEEE 802.11 wireless mesh networks," *IEEE Trans. Wireless Commun.*, vol. 8, no. 1, pp. 166–175, Jan. 2009.

[18] G. H. E. Fard, M. H. Yaghmaee, and R. Monsefi, "An adaptive cross-layer multichannel QoS-MAC protocol for cluster based wireless multimedia sensor networks," in *Proc. ICUMT Workshops*, Oct. 12–14, 2009, pp. 1–6.

[19] Y.-F. Wen and W. Liao, "On QoS routing in wireless ad-hoc cognitive radio networks," in *Proc. IEEE 71st VTC*, May 16–19, 2010, pp. 1–5.

[20] L. Ding, T. Melodia, S. N. Batalama, J. D. Matyjas, and M. J. Medley, "Cross-layer routing and dynamic spectrum allocation in cognitive radio ad hoc networks," *IEEE Trans. Veh. Technol.*, vol. 59, no. 4, pp. 1969–1979, May 2010.

[21] K. R. Chowdhury and M. D. Felice, "SEARCH: A routing protocol for mobile cognitive radio ad-hoc networks," *Comput. Commun.*, vol. 32, no. 18, pp. 1983–1997, Dec. 2009.

[22] G.-M. Zhu, I. F. Akyildiz, and G.-S. Kuo, "STOD-RP: A spectrum-tree based on-demand routing protocol for multi-hop cognitive radio networks," in *Proc. IEEE GLOBECOM*, Nov. 2008, pp. 1–5.

[23] H. Zhao, E. Garcia-Palacios, J. Wei, and Y. Xi, "Accurate available bandwidth estimation in IEEE 802.11-based ad hoc networks," *Comput. Commun.*, vol. 32, no. 6, pp. 1050–1057, Apr. 2009.

[24] K. Stuhlmuller, N. Farber, M. Link, and B. Girod, "Analysis of video transmission over lossy channels," *IEEE J. Sel. Areas Commun.*, vol. 18, no. 6, pp. 1012–1032, Jun. 2000.

[25] T. Wiegand and G. J. Sullivan, "The H.264/AVC video coding standard," *IEEE Signal Process. Mag.*, vol. 24, no. 2, pp. 148–153, Mar. 2007.
[26] H. Kim and K. G. Shin, "Efficient discovery of spectrum opportunities with MAC-layer sensing in cognitive radio networks," *IEEE Trans. Mobile Comput.*, vol. 7, no. 5, pp. 533–545, May 2008.
[27] L. Zhou, X. Wang, W. Tu, G. Mutean, and B. Geller, "Distributed scheduling scheme for video streaming over multi-channel multi-radio multi-hop wireless networks," *IEEE J. Sel. Areas Commun.*, vol. 28, no. 3, pp. 409–419, Apr. 2010.
[28] A. A. Abbasi and M. Younis, "A survey on clustering algorithms for wireless sensor networks," *Comput. Commun.*, vol. 30, no. 14/15, pp. 2826–2841, Oct. 2007.
[29] A. Lie and J. Klaue, "Evalvid-RA: trace driven simulation of rate adaptive MPEG-4 VBR video," *Multimedia Syst.*, vol. 14, no. 1, pp. 33–50, Jun. 2008.
[30] V. Mhatre and C. Rosenberg, "Design guidelines for wireless sensor networks: communication, clustering and aggregation," *Ad Hoc Netw.*, vol. 2, no. 1, pp. 45–63, Jan. 2004.
[31] F. Digham, M. Alouini, and M. Simon, "On the energy detection of unknown signals over fading channels," in *Proc. IEEE ICC*, 2005, vol. 5, pp. 3575–3579.
[32] The Network Simulator-ns-2. [Online]. Available: http://www.isi.edu/nsnam/ns/
[33] Cognitive Radio Network patch for ns2. [Online]. Available: https://docs.google.com/file/d/0B7S255p3kFXNNXEtS3ozTHpmRHM/edit

Ghalib A. Shah (M'09) received the Ph.D. degree in computer engineering from Middle East Technical University, Ankara, Turkey, in 2007.

He then joined the College of Electrical and Mechanical Engineering, National University of Sciences and Technology, Islamabad, Pakistan, as an Assistant Professor. From 2009 to 2010, he was a Visiting Fellow with the School of Computer Science, Australian National University, Canberra, Australia. He later joined the Center for Advanced Research in Engineering, Islamabad, as a member of the technical staff and led various networking projects. He is currently an Associate Professor with the Al-Khawarizmi Institute of Computer Science, University of Engineering and Technology Lahore, Lahore, Pakistan. He is the author of several papers in well-recognized conferences and journals. His research interests include the design and analysis of communication protocols from medium access control to transport layer for cognitive radio networks, wireless multimedia networks, Internet of Things, and software-defined networks.

Dr. Shah received an OIC Standing Committee on Scientific and Technological Cooperation—The Academy of Sciences for the Developing World joint research grant for young researchers.

Fatih Alagoz (M'01) received the B.Sc. degree from Middle East Technical University, Ankara, Turkey, in 1992 and the M.Sc. and D.Sc. degrees from The George Washington University, Washington, DC, USA, in 1995 and 2000, respectively, all in electrical engineering.

He is currently a Professor with the Department of Computer Engineering, Boğaziçi University, Istanbul, Turkey. He has contributed to many research projects for various agencies/organizations, including the U.S. Army Intelligence Center, the Naval Research Laboratory, the United Arab Emirates Research Fund, the Turkish Scientific Research Council, and the State Planning Organization of Turkey. He is the Satellite Systems Advisor to the Kandilli Earthquake Research Institute, Istanbul. He is an editor of five books and an author of more than 100 scholarly papers in selected journals and conferences. His research interests include wireless/mobile/satellite communication networks.

Dr. Alagoz is a member of the IEEE Satellite and Space Communications Technical Committee. He has served on several major conference technical committees and organized and chaired technical sessions at many international conferences. He has received numerous professional awards.

Etimad A. Fadel received the B.S. degree in computer science from King Abdulaziz University (KAU), Jeddah, Saudi Arabia, in 1994, with a senior project titled *ATARES: Arabic Character Analysis and Recognition*, and the M.Phil/Ph.D. degree in computer science from De Montfort University, Leicester, U.K., in 2007, with a thesis titled *Distributed Systems Management Service*.

She is currently an Assistant Professor with the Department of Computer Science, KAU. Her main research interests include distributed systems, which are developed based on middleware technology. Her current research interests include wireless networks, Internet of Things, and Internet of Nano-Things.

Ozgur B. Akan (M'00–SM'07) received the B.Sc. degree in electrical and electronics engineering from Bilkent University, Ankara, Turkey, in 1999; the M.Sc. degree in electrical and electronics engineering from Middle East Technical University, Ankara, in January 2002; and the Ph.D. degree in electrical and computer engineering from Georgia Institute of Technology, Atlanta, GA, USA, in May 2004.

From May 2004 to August 2010, he was with the Department of Electrical and Electronics Engineering, Middle East Technical University. He is currently a Full Professor with the Department of Electrical and Electronics Engineering, Koç University, Istanbul, Turkey, where he is also the Director of the Next-Generation and Wireless Communications Laboratory. His current research interests include nanoscale, molecular, and quantum communications; next-generation wireless communications; cognitive radio networks; sensor networks; satellite and space communications; underwater acoustic communications; signal processing for communications; and information theory.